DETERMINATION OF IN-SITU PERMEABILITY FROM TUBE WAVE VELOCITY AND ATTENUATION

by

D.R. Burns and C.H. Cheng

Earth Resources Laboratory
Department of Earth, Atmospheric, and Planetary Sciences
Massachusetts Institute of Technology
Cambridge, MA 02139

ABSTRACT

Recent investigations by a number of different authors have shown that the phase velocity and attenuation of the tube (Stoneley) wave in the borehole is correlated with *in situ* permeability. Specifically, velocity decreases and attenuation increases as a function of *in situ* permeability. Hsui et al. (1985) presented two theoretical models relating *in situ* permeability to tube wave attenuation. The results obtained from one of the models, the modified Biot-Rosenbaum model, agreed well with the data of Williams et al. (1984). We have extended the results from the modified Biot-Rosenbaum model to examine the relationship between tube wave velocity and *in situ* permeability. It is found that with an open borehole Biot-Rosenbaum model, i.e., allowing for the communication between the pore and borehole fluid pressures, we can match the variation of tube wave phase velocity with *in situ* permeability in the data presented by Williams et al. and by Zemanek et al. (1985). Furthermore, by the introduction of intrinsic attenuation, i.e., attenuation not caused by Biot fluid flow mechanism, we can fit both the velocity and attenuation data simultaneously. Williams et al. had also observed that the existence of a mudcake did not appear to significantly affect the observed correlation of tube wave velocity and attenuation with permeability. In the Biot-Rosenbaum model, this is explained by the fact that a mudcake is not rigid, and there can be communication between the pore and borehole fluid pressure systems without actual fluid exchange between them. Thus if one can determine the formation P- and S-wave velocity and attenuation, the *in situ* permeability may be obtainable using the Biot-Rosenbaum model.

BACKGROUND

The estimation of *in situ* permeability from borehole geophysical logs has been a topic of discussion for the past 30 years. Empirical relations between porosity and permeability provide reasonable estimates when applied to particular rock types in specific geographic regions. Simple capillary tube models of a permeable rock, such as the Carman-Kozeny model, have also been investigated in detail. Such models relate permeability to porosity

and formation factor, two measurable quantities, and the hydraulic radius (the ratio of pore volume to pore surface area) which cannot be measured *in situ*. The Carman-Kozeny model has been used to predict permeability with some success (Brace, 1977) but is difficult to apply to the *in situ* estimation problem. A more promising approach utilizes the tube wave portion of the full waveform acoustic log. Williams et al. (1984) and Zemanek et al. (1985) have shown significant correlations between core measured permeabilities and the tube wave velocity and attenuation. Their results indicate that over a fairly wide range of permeabilities (0.01 – 3000 md) the tube wave velocity and attenuation can provide an estimate of the relative permeability variations as a function of depth in the borehole. All other factors being equal, the tube wave velocity decreases and the attenuation increases with increasing permeability. The tube wave velocity, however, is also sensitive to any changes in the formation shear wave velocity due to lithologic variations. The tube wave attenuation, in addition to being sensitive to the formation permeability, is also affected by other attenuation mechanisms (we will use the term 'intrinsic attenuation') which must be accounted for. In order to fully understand the effects of all these factors on the tube wave velocity and attenuation, a theoretical model of tube wave propagation which includes the effects of permeability is needed. An appropriate model would also provide the means for estimating the *in situ* permeability in an absolute sense from tube wave measurements.

Biot (1956a, b) developed a theoretical model for wave propagation in a porous solid containing a viscous pore fluid. In this model, the permeability of the solid is a necessary parameter to describe the relative motion between the solid matrix and the pore fluid. Such motion results in attenuation of any propagating seismic waves. Rosenbaum (1974) applied the Biot model to the full waveform acoustic logging problem by assuming that the borehole was surrounded by a porous Biot solid. Although this formulation treats the attenuation due to fluid motion (and therefore permeability), it does not treat any other attenuation mechanisms (such as friction or grain boundary relaxation). Rosenbaum (1974) did investigate the attenuation of the tube wave as a function of permeability, but did not look at tube wave velocity effects. The use of a high frequency source in his synthetic studies, however, resulted in poor tube wave excitation, and, therefore, the tube wave sensitivity to permeability changes was not fully appreciated. White (1983) investigated the effects of a permeable formation on tube wave velocity and attenuation by looking at a low frequency approximation to the problem. His results, based on a simplified borehole wall impedence function, showed that the tube wave velocity and attenuation should be sensitive to permeability changes at low frequencies. Hsui et al. (1985) used the approach of White (1983) and Rosenbaum (1974) to study tube wave attenuation as a function of permeability. They also modified the Rosenbaum formulation by introducing complex velocities to treat the effects of intrinsic attenuation. The results of this modified Biot-Rosenbaum model agree well with the data of Williams et al. (1984). Hsui et al. (1985) did not investigate the effects of permeability on tube wave velocity. Schmitt et al. (1985) have also used a modified Biot-Rosenbaum type formulation in full waveform acoustic log studies, but they have concentrated on the effects of pore shape and tortuosity on the permeability factor in the Biot model and have not addressed the permeability estimation problem.

In this paper, we have extended the results of Hsui et al. (1985) by using the modified Biot-Rosenbaum model to study the tube wave velocity as well as attenuation. In addition to comparing the model to the the data of Williams et al. (1984), we also compare the model results to the data of Zemanek et al. (1985) which illustrate the relative effects of lithologic and permeability variations on the tube wave velocity.

RESULTS AND DISCUSSION

In this section we will begin by discussing the theoretical results of the modified Biot-Rosenbaum model. In all of the results presented in this section, the borehole fluid and pore fluid are assumed to be in total communication. Figure 1a shows the predicted tube wave phase velocity and attenuation as a function of permeability for frequencies of 1, 2, and 5 kHz. The model parameters for this figure and all others are given in Table 1. As seen in this figure, the tube wave phase velocity decreases with increasing permeability, although the phase velocity becomes less sensitive to permeability as the frequency increases. The increase in phase velocity at high permeability for the 5 kHz case is related to the transition from the low frequency to high frequency region in the Biot model (Biot, 1956a, b). The tube wave attenuation (Figure 1b) appears to be much more sensitive to changes in the permeability. The attenuation of the tube wave increases quite dramatically with increasing permeability, although the effect diminishes with increasing frequency. It should also be noted that below about 10 md, the tube wave velocity and attenuation show very little change with permeability.

In order to illustrate the effect of intrinsic attenuation on the tube wave, we have plotted the attenuation (inverse of the quality factor Q) as a function of frequency for the same formation used in Figure 1 with permeability values of 100 md (Figure 2a) and 1000 md (Figure 2b). In the lower permeability case (100 md), the intrinsic attenuation is the dominant factor except at very low frequencies. In the high permeability case (1000 md), the fluid flow or permeability related attenuation is the dominant factor. It should be noted that the intrinsic attenuation component generally adds a constant shift to the attenuation resulting from fluid flow.

In the remainder of this section, the theoretical model results will be compared to the published data of Williams et al. (1984) and Zemanek et al. (1985). Williams et al. (1984) presented data from three wells which compared the tube wave velocity and attenuation to smoothed core permeability measurements. Although they did include the P-wave travel time log for each well, they did not include any information on the formation shear wave velocity, and only provided ranges of porosity values. Based on such limited information, we can only attempt to estimate the parameters necessary for the model calculations. The data set of Zemanek et al. (1985) is much more complete since it includes both the P- and S-wave travel time curves as well as a gamma ray log. The parameters used to generate the theoretical results for each of the four data sets (3 from Williams et al. and 1 from Zemanek et al.) are given in Table 1. It

should also be emphasized that core permeability measurements can vary from *in situ* permeability values (as measured by a packer test, for example) by as much as two orders of magnitude (Brace, 1977). Large scale conduits in the formation result in higher *in situ* permeabilities while fractured or damaged cores give the opposite result. Thus the results in this paper should be viewed in that light.

The first data sets we will examine are from Williams et al. (1984). These data sets will be referred to as well 1, well 2, and well 3 which correspond to the convention used in Williams et al. (1984). In all three of these wells, only limited information was provided – the compressional wave velocity of the formation, the smoothed permeability values, the general lithology of the permeable zone, and the porosity range. In order to make calculations of tube wave velocity and attenuation with the theoretical model, the compressional and shear wave velocity of the formation (these velocities should correspond to the dry or frame velocities), the matrix density, the porosity, the pore fluid density, velocity, and viscosity, and the borehole fluid density and velocity are required. By necessity, several parameters had to be estimated in order to generate theoretical results for these three wells. In all three cases, all parameters except permeability were assumed to be constant. The formation and borehole fluid quality factors (corresponding to intrinsic attenuation) for each well have been chosen to provide the best fit with the measured tube wave attenuation values. The parameter values are given in Table 1.

Figure 3 shows the data from well 1 given in Williams et al. (1984). The formation in this well is a fairly low permeability fractured limestone. The P-wave velocity is estimated from the given log, and the formation S-wave velocity is chosen to give a V_p/V_s ratio of 2. The borehole fluid velocity is assumed to be 1.53 km/sec. The porosity is taken to be 20% based on the reported porosity variation of 0–20% over the entire interval. The matrix density is taken as 2.72 g/cc which results in a formation density of 2.38 g/cc. Included in this figure are the P-wave travel time log, the tube wave amplitude ratio log, and the tube wave travel time log, each superimposed with the smoothed core permeability measurements. Mobil's long spaced acoustic log (LSAL), which was used to generate this data, has a receiver separation of 5 feet, so Williams et al. (1984) used a 5 foot average of the core permeability values to generate the permeability curves in their paper. The amplitude ratio curve represents the ratio of the energy contained in the first cycle of the tube wave from the far and near receivers. The tube wave frequency for this data was reported to be about 5 kHz. The amplitude ratio and tube wave travel time curves appear to be very sensitive to changes in permeability in this example. The model results are represented by the solid dots in Figure 3. These results correspond to the calculated tube wave amplitude ratio and travel time based on the given permeability variations. Although there is good agreement between the data and model results, the model results are not as sensitive to the permeability variations as the data appear to be. This is not too surprising since the permeability values in this well are quite low, ranging between 1 and 10 md. As we illustrated in Figure 1, the model is insensitive to permeability values less than about 10 md. In this particular well it is likely that the measured tube wave variations are due to lithologic variations which result in changes in the shear wave velocity of the formation. This hypothesis

is supported by the P-wave travel time curve shown in Figure 3. This curve shows variations in P-wave velocity of 5–10% within the permeable interval. It is likely that the shear wave velocity varies by a similar amount which could explain the tube wave velocity variations which were measured. Variations in the lithology could also result in changes in the intrinsic attenuation values of the formation which would affect the measured tube wave amplitude ratio. It appears, then, in this well that the tube wave variations are due to changes in lithology which are also controlling the permeability variations.

In Figure 4, the data and results for well 2 of Williams et al. (1984) are presented. The formation in this example is an interbedded oolitic limestone and sandstone at the top and bottom, with poor porosity and permeability, and a section of increased sandiness in the middle with a corresponding increase in porosity and permeability. Only this higher permeability zone is used in the theoretical model calculations. In this zone, the porosity is assumed to be 25%, the matrix density is taken to be 2.70 g/cc, and the P- and S-wave velocities are estimated in the same manner as well 1. The tube wave frequency is 5 kHz. As in the well 1 example, the tube wave measurements appear to correlate quite well with the permeability measurements. The model results are in good agreement with the measurements, although the sensitivity to permeability variations is somewhat weak. The insensitivity of the model results is generally due to the low permeability values in much of the well (permeabilities range from about 0.1 to 100 md although most of the values fall below 10 md). As in the well 1 example, the P-wave velocity log shows some variation over the permeable zone which indicates that lithologic variations may play some role in the measured tube wave variations. Williams et al. (1984) also stated that a thick (3/4") mudcake was present in this well that did not appear to hinder the tube wave sensitivity to permeability. This indicates that although a mudcake may not permit actual fluid flow from the borehole to the formation due to the passing tube wave, it does allow the borehole fluid pressure to be transmitted to the pore fluid of the formation.

The final example from Williams et al. (1984) is well 3. This formation consists of a sandstone sequence which ranges from well consolidated to unconsolidated and is highly permeable (permeability ranges from about 10 to over 3000 md). This formation has a shear wave velocity which is less than the borehole fluid velocity which results in a much lower tube wave frequency (1.5 kHz in this case). The porosity was assumed to be 30% and the matrix density 2.65 g/cc. The data and model results for this well are shown in Figure 5. The correlations between the measured tube wave amplitude ratio and travel time and the permeability variations are excellent. The model results in this case agree very well with the measured tube wave parameters and also appear to be very sensitive to the permeability variations. The P-wave travel time log (Figure 5) indicates that although there may be some slight lithologic variations in this interval, these variations are not responsible for the wide range of tube wave velocity and attenuation values that have been measured. The results for this well indicate that the theoretical model appears to be adequately representing the effect of permeability on the tube wave. This well provides good results for several reasons. First, the permeability range is quite

high and falls into the region in which the theory predicts that the tube wave should be very sensitive to permeability changes (Figure 1). Second, the frequency of the tube wave is much lower in this example because the formation shear wave velocity is lower than the borehole fluid velocity (slow formation). As previously discussed, the theory predicts that the tube wave is much more sensitive to permeability variations at lower frequencies (Figure 1). Finally, it appears that any lithologic variations in the formation in this well are too small to explain the tube wave velocity and attenuation variations that have been measured, meaning that the fluctuations in tube wave measurements are almost totally related to the effects of permeability.

The last example to be treated is the limestone/shale sequence data from Zemanek et al. (1985) which we will refer to as well 4. In this well, both the P-wave and S-wave travel time logs are available which allow us to compare the effects of lithologic variations and the effects of permeability variations on the tube wave velocity. In this example, the tube wave attenuation was not reported. Figure 6 shows the P-wave and S-wave travel time logs and the gamma ray log over the interval of interest. We will focus on the interval between the depths of 1800 and 1900. In this interval, two shale zones exist at depths of about 1800 and 1875 as seen on the gamma ray log and the P- and S-wave travel time logs (slow velocities). Between these shale beds is a limestone unit with what appears to be a porous zone between depths of about 1825 and 1850. This porous zone corresponds to a permeable limestone unit; to either side of this unit is a limestone of low porosity and permeability. Figure 7 shows the measured tube wave travel time and smoothed core permeability values over the interval from 1800 to 1900. The tube wave travel time correlates well with the permeability values, but there are also large variations in the travel time corresponding to the lithologic changes from limestone to shale.

In order to test the theoretical model on this well, we will first try to model the tube wave velocity variations due to lithology. To accomplish this, the tube wave velocity is calculated for the elastic case only, that is, with no permeability effects included. In order to perform this calculation, the formation P-wave and S-wave velocity and density, the borehole fluid velocity and density, and the radius of the borehole are needed. The formation velocities are available from the logs given in Zemanek et al. (1985), and the formation density has been estimated by assuming that the shale density is 2.5 g/cc, the impermeable (zero porosity) limestone density is 2.7 g/cc, and the permeable limestone density is 2.28 g/cc. The permeable limestone density is based on a matrix density of 2.7 g/cc and a porosity of 25% (based on the time average equation applied to the P-wave travel time in this interval). The borehole radius is assumed to be 10 cm, the borehole fluid velocity is set at 1.54 km/sec, and the borehole fluid density is taken to be 1.4 g/cc. The calculated elastic tube wave travel times are compared to the measured values in Figure 8 (the elastic values are given by the dashed line). The calculated elastic values agree very well with the measured values, but the measured values are about 3% greater (slower velocity) in the permeable interval between 1825 and 1850. The calculated travel time for the shale bed at a depth of 1800 is about 5% greater than the measured value which may be due to a slight washout of the borehole in

this zone, or an incorrect density being assumed. The difference between the measured values and the calculated values in the permeable zone should correspond to the effect of permeability. The solid dots in Figure 8 correspond to the calculated tube wave velocity using the modified Biot-Rosenbaum model and the measured permeability values given in Figure 7. The permeability effect explains most of the increased travel time in the limestone interval between 1825 and 1850. These results indicate that the elastic tube wave calculations can explain the lithologic effects on the tube wave velocity (as can be seen in the shale zones and the impermeable limestone units), but that these calculations cannot fully explain the slower tube wave velocity that exists in the permeable zone. Even the calculations with the modified Biot-Rosenbaum model do not fully explain the measured travel time data. However if the pore fluid contains any gas, or if the viscosity of the pore fluid is lower than the assumed value (0.4 cP), a better fit is possible. It should also be noted that there are no major lithologic variations within this permeable interval, with the possible exception of a shale stringer at about 1835, as seen on the gamma ray log (Figure 6).

CONCLUSIONS

The modified Biot-Rosenbaum model can be used to explain the effect of permeability on tube wave velocity and attenuation for permeability values between about 10 and 3000 md. The tube wave is also affected by variations in lithology which must be accounted for before any attempt at permeability estimation is undertaken. The model also indicates that tube wave sensitivity to permeability increases as frequency decreases. It appears that if the formation P-wave and S-wave velocities and attenuation can be determined, then the *in situ* permeability can be estimated from this model. Although the tube wave velocity is easier to measure than the tube wave attenuation, it is not as sensitive to permeability variations, so both parameters should be used.

ACKNOWLEDGEMENT

The work was supported by the Full Waveform Acoustic Logging Consortium at M.I.T. D.R. Burns was partially supported by a Phillips Petroleum Fellowship.

REFERENCES

Biot, M.A., 1956a, Theory of propagation of elastic waves in a fluid saturated porous rock: I. Low frequency range; J. Acoust. Soc. Am., 28, 168-178.

Biot, M.A., 1956b, Theory of propagation of elastic waves in a fluid saturated porous

rock: II. Higher frequency range; J. Acoust. Soc. Am., 28, 179-191.

Brace, W.F., 1977, Permeability from resistivity and pore shape; J. Geophys. Res., 82, 3343-3349.

Hsui, Albert T., Zhang, J., Cheng, C.H., and Toksöz, M.N., 1985, Tube wave attenuation and in-situ permeability; Trans. SPWLA 26th Ann. Log. Symp., Paper CC.

Rosenbaum, J.H., 1974, Synthetic microseismograms: logging in porous formations; Geophysics, 39, 14-32.

Schmitt, D.P., Bouchon, M., and Bonnet, G., 1985, Influence of viscous and mass coupling coefficients when logging in saturated porous formations; abstract, SEG 55th Ann. Meeting.

White, J.E., 1983, Underground Sound; Elsevier, Holland.

Williams, D.M., Zemanek, J., Angona, F.A., Dennis, C.L., and Caldwell, R.L., 1984, The long space acoustic logging tool; Trans. SPWLA 25th Ann. Log. Symp., Paper T.

Zemanek, J., Williams, D.M., Caldwell, R.L., Dennis, C.L., and Angona, F.A., 1985, New developments in acoustic logging; presented at the Indonesian Petroleum Assoc. 14th Ann. Conv.

TABLE 1: Parameters used in this study

FIGURE	V_p km/s	V_s km/s	V_f km/s	ρ g/cm^3	ρ_f g/cm^3	Q_p	Q_s	Q_f	ϕ %	Permeability md
1	3.80	2.20	1.50	2.65	1.00	∞	∞	∞	15	
2a	3.80	2.20	1.50	2.65	1.00	100	50	20	15	100
2b	3.80	2.20	1.50	2.65	1.00	100	50	20	25	1000
3	5.00	2.50	1.53	2.72	1.00	100	60	35	20	
4	3.20	1.60	1.53	2.70	1.00	100	50	15	25	
5	3.37	1.49	1.53	2.65	1.00	25	12	10	25	
8	4.15	2.45	1.54	2.70	1.40	∞	∞	∞	25	

Please note that all formation velocities are "frame" or dry velocities.

The viscosity of the pore fluid is 1.0 centipoise, except in Figure 8, where a value of 0.4 centipoise is used.

Biot's structural constant is $\sqrt{8}$, Morse's dynamic fluid-solid coupling factor is 3.

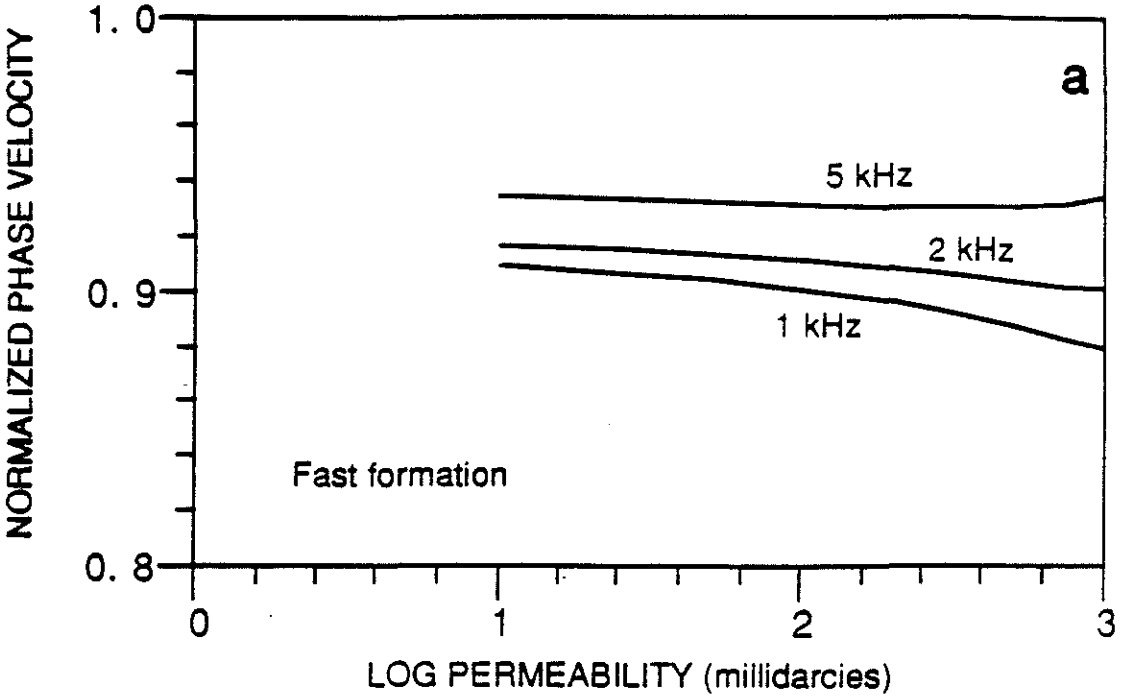

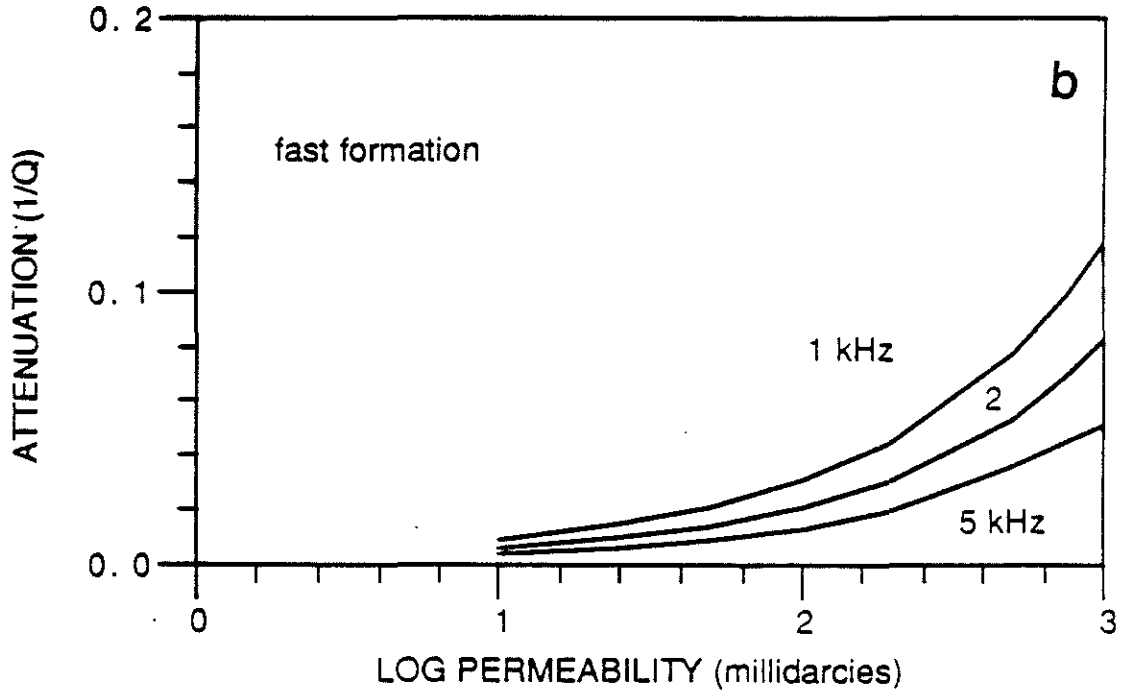

Figure 1: Tube wave (a) phase velocity and (b) attenuation (1/Q) as a function of permeability for a 15% porosity sandstone for 3 different frequencies.

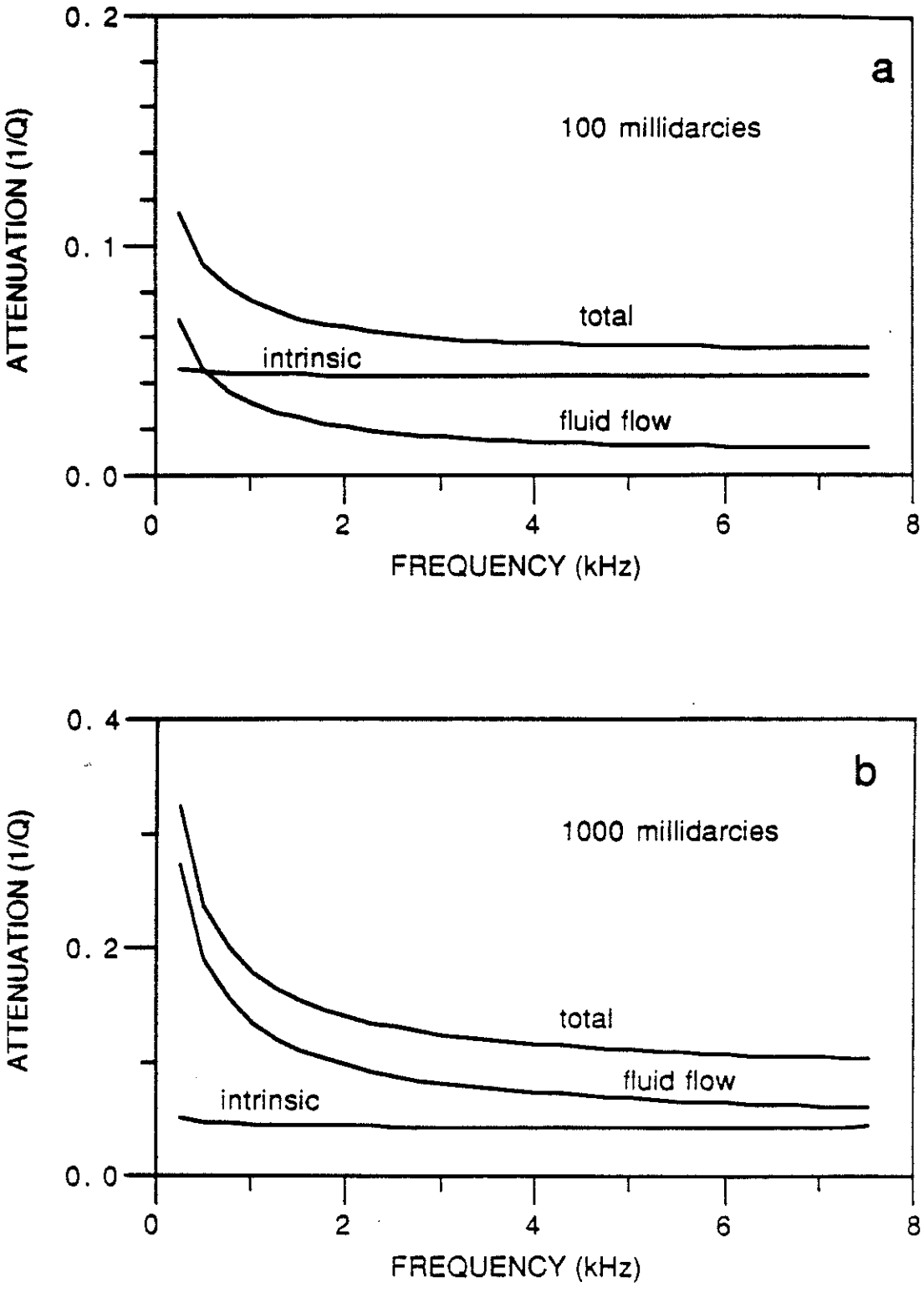

Figure 2: Tube wave attenuation (1/Q) versus frequency for (a) a formation with a porosity of 15% and a permeability of 100 millidarcies and (b) a formation with a porosity of 25% and a permeability of 1000 millidarcies. Total attenuation is the sum of intrinsic attenuation and attenuation due to fluid flow.

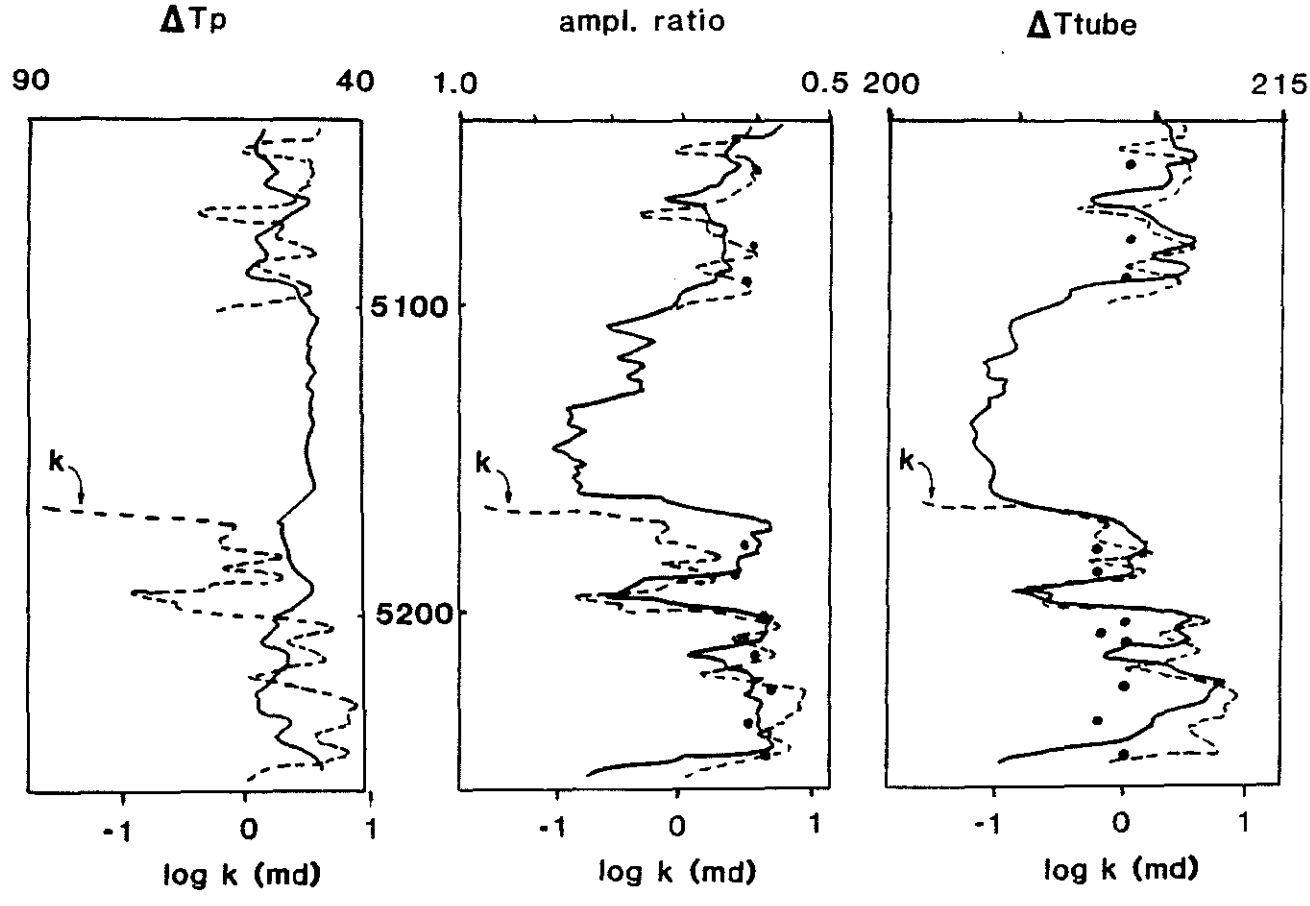

Figure 3: The compressional travel time, tube wave amplitude ratio, and tube wave travel time logs for well 1 from Williams et al. (1984). Each log has the smoothed core permeability values superimposed (dashed line). The predicted tube wave amplitude ratio and travel time based on the modified Biot-Rosenbaum model are given by the solid dots. The parameters used to generate the theoretical results are given in Table 1.

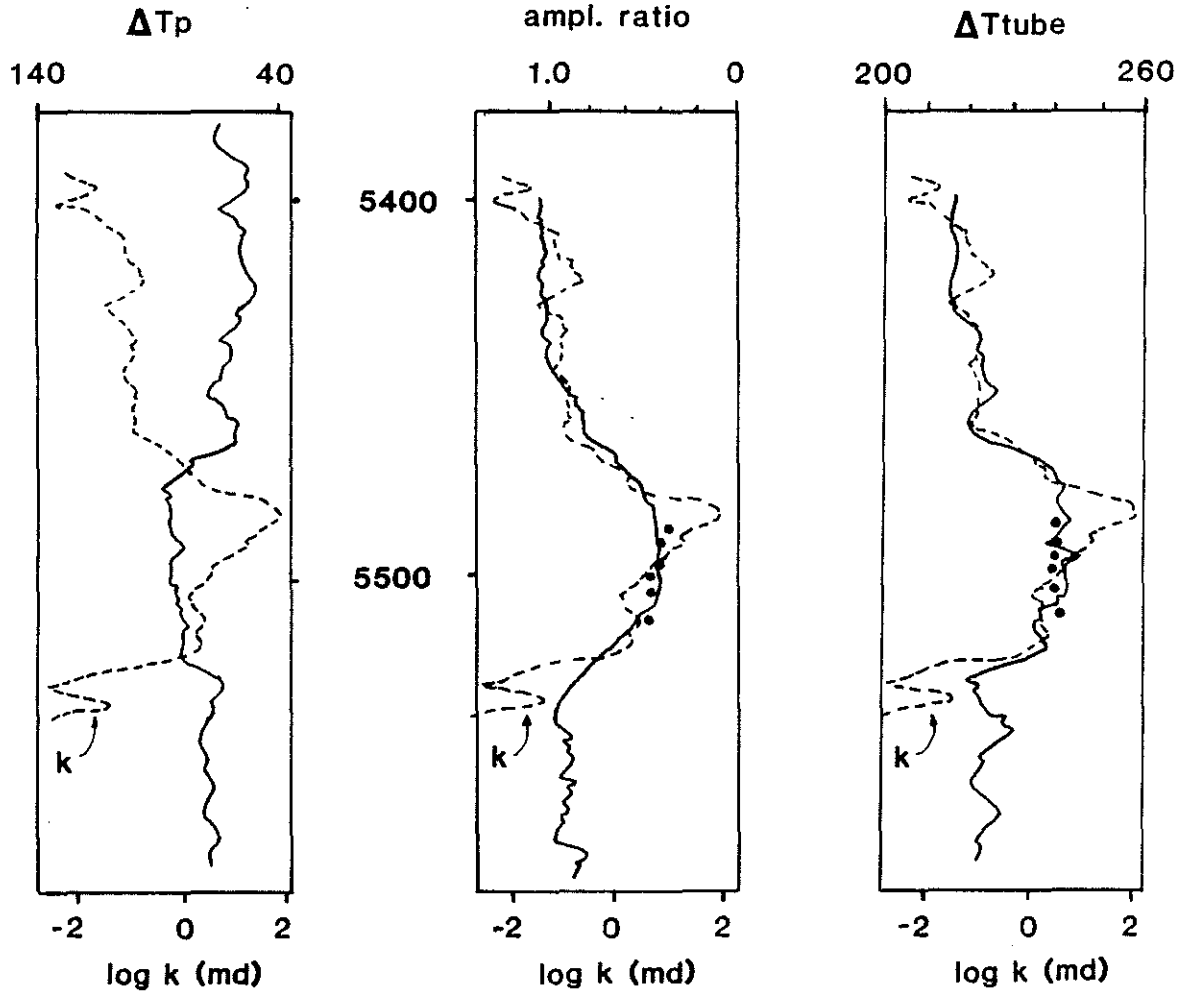

Figure 4: The compressional travel time, tube wave amplitude ratio, and tube wave travel time logs for well 2 from Williams et al. (1984). Each log has the smoothed core permeability values superimposed (dashed line). The predicted tube wave amplitude ratio and travel time based on the modified Biot-Rosenbaum model are given by the solid dots. The parameters used to generate the theoretical results are given in Table 1.

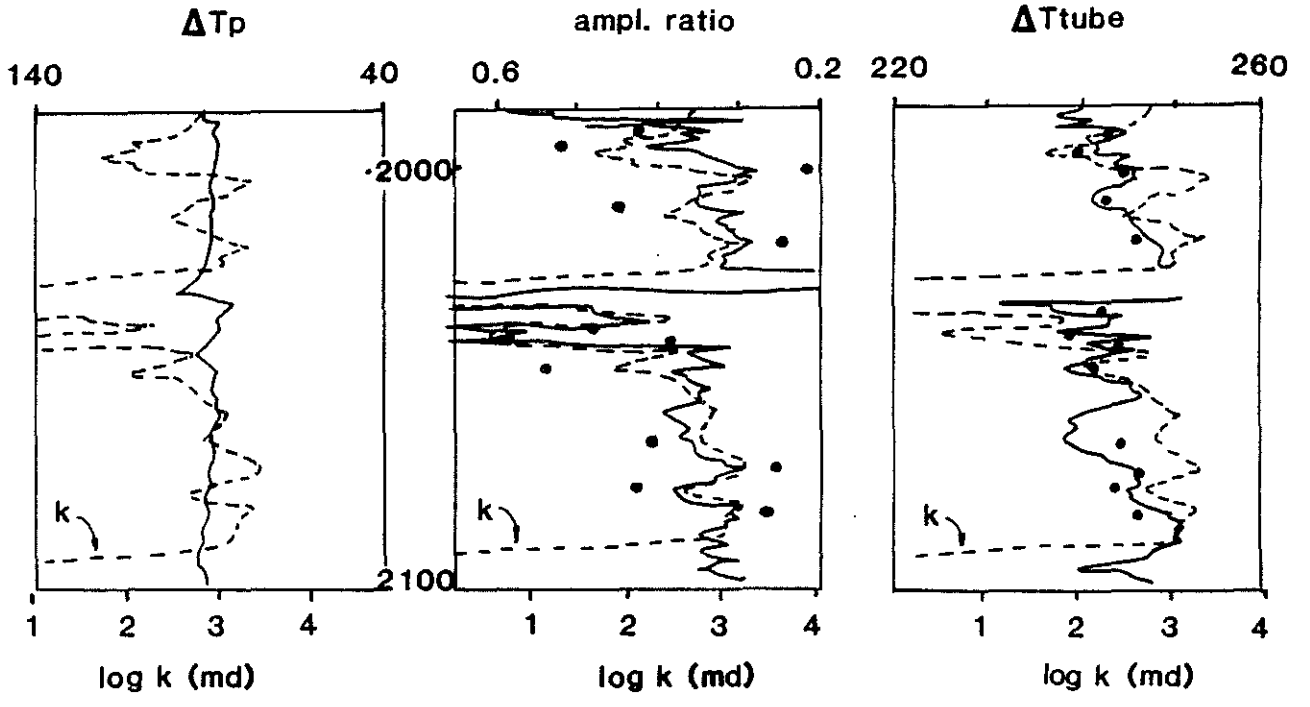

Figure 5: The compressional travel time, tube wave amplitude ratio, and tube wave travel time logs for well 3 from Williams et al. (1984). Each log has the smoothed core permeability values superimposed (dashed line). The predicted tube wave amplitude ratio and travel time based on the modified Biot-Rosenbaum model are given by the solid dots. The parameters used to generate the theoretical results are given in Table 1.

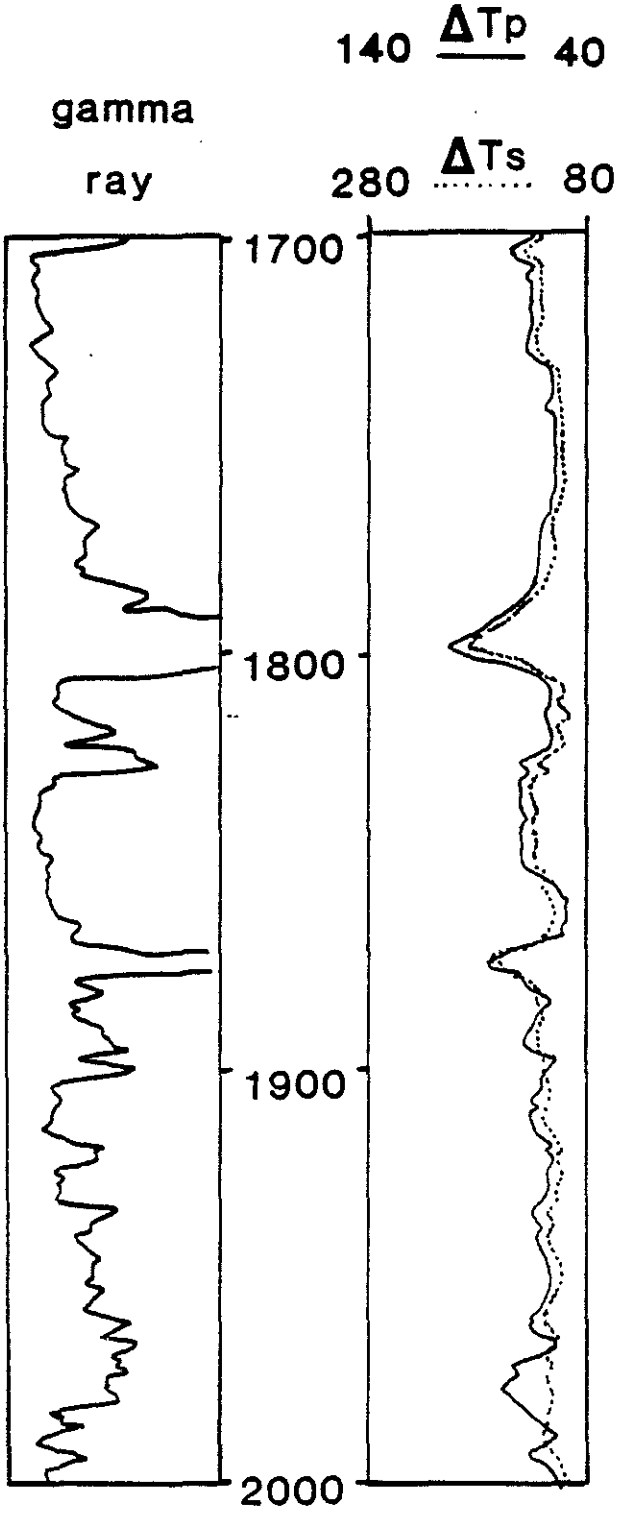

Figure 6: The gamma ray log and compressional and shear wave travel time logs for well 4 from Zemanek et al. (1985).

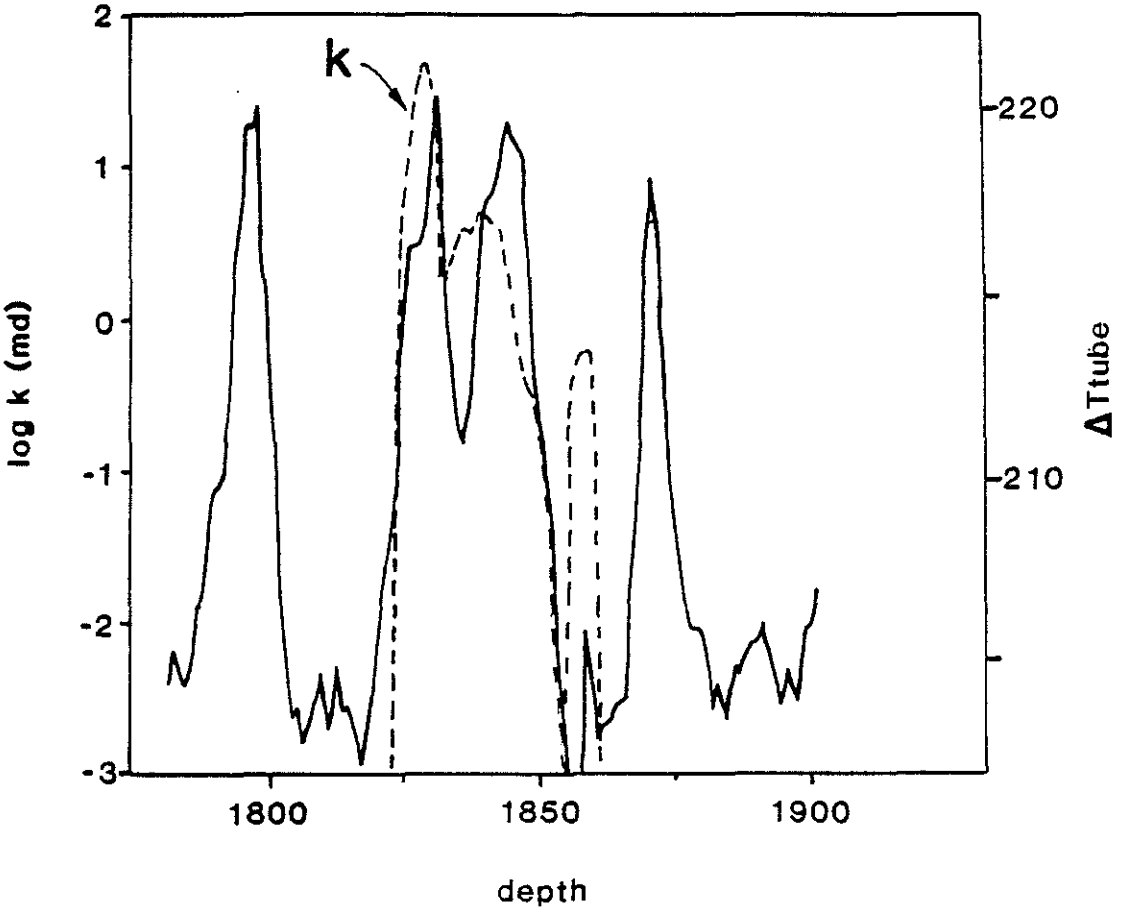

Figure 7: The tube wave travel time for the interval between the depths of 1800 and 1900 in well 4 from Zemanek et al. (1985). The smoothed core permeability values are also included (dashed curve).

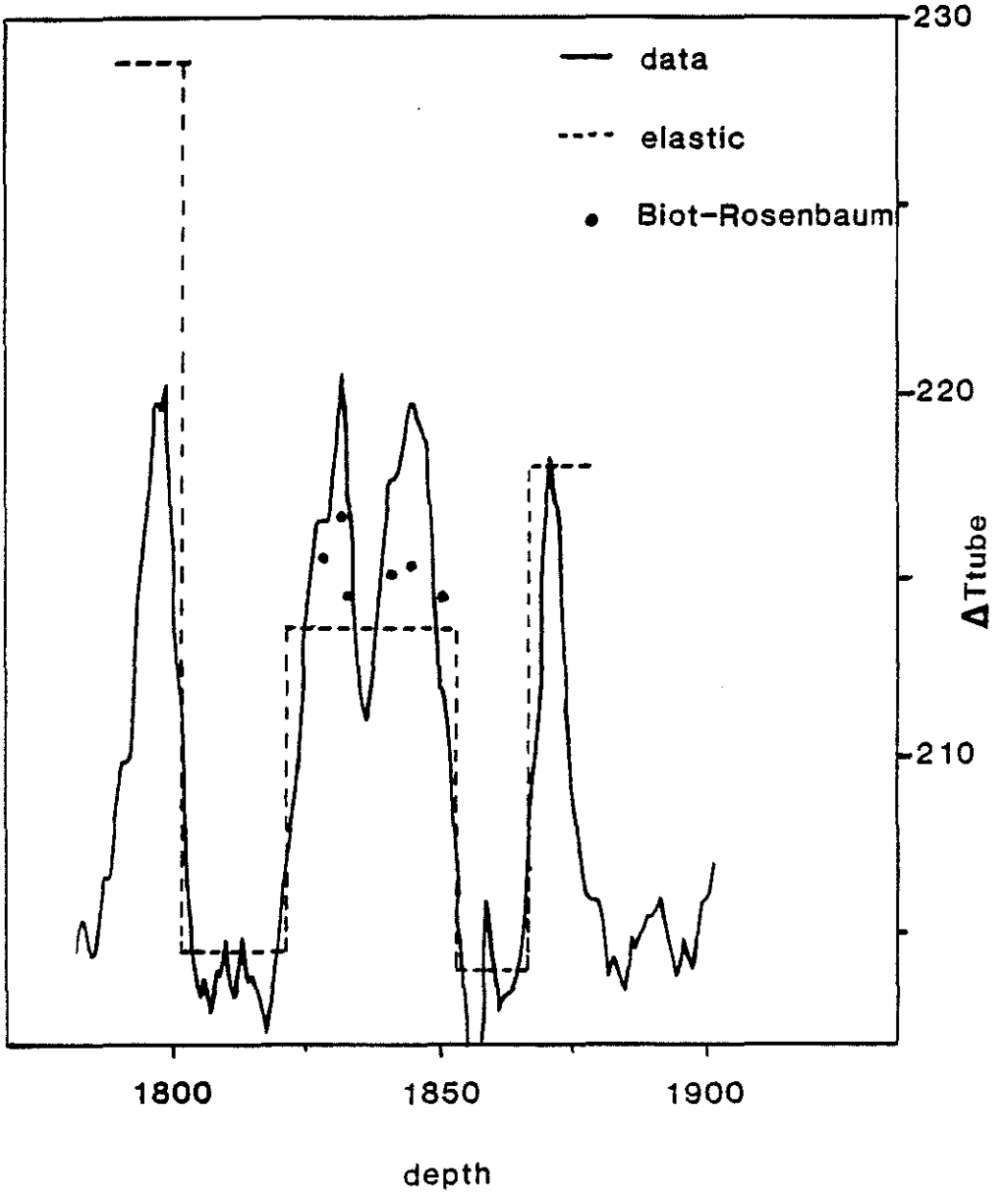

Figure 8: The tube wave travel time curve from well 4 from Zemanek et al. (1985). The dashed line represents the calculated tube wave travel time for the elastic case (no permeability effects), and the solid dots represent the calculated tube wave travel time using the modified Biot-Rosenbaum model to account for the effects of permeability. The parameters used in the Biot-Rosenbaum calculations are given in Table 1.